Physics Letters B 703 (2011) 633–640

Contents lists available at SciVerse ScienceDirect

Physics Letters B

www.elsevier.com/locate/physletb

Holographic multi-band superconductor

Ching-Yu Huang [a], Feng-Li Lin [a,*], Debaprasad Maity [b,c]

[a] Department of Physics, National Taiwan Normal University, Taipei 116, Taiwan
[b] Department of Physics and Center for Theoretical Sciences, National Taiwan University, Taipei 106, Taiwan
[c] Leung Center for Cosmology and Particle Astrophysics, National Taiwan University, Taipei 106, Taiwan

ARTICLE INFO

Article history:
Received 23 July 2011
Accepted 18 August 2011
Available online 24 August 2011
Editor: T. Yanagida

Keywords:
AdS/CFT
Holographic superconductor
Two-band superconductor

ABSTRACT

We propose a gravity dual for the holographic superconductor with multi-band carriers. Moreover, the currents of these carriers are unified under a global flavored SO(3) symmetry, which is dual to the bulk SO(3) gauge symmetry. We study the phase diagram of our model, and find it qualitatively agrees with the one for the realistic 2-band superconductor, such as MgB_2. We also identify the bulk field dual to the electromagnetic $U(1)_{EM}$ current, which should be invariant under the global flavored SO(3) rotation. We then evaluate the corresponding holographic conductivity and find the expected mean field like behaviors.

1. Introduction

Symmetry principle is believed to be one of the important guiding principles in constructing the new physics models. As is well known in the context of standard model of particle physics, some non-trivial dynamics could be unified in the form of non-Abelian symmetry, such as gauge symmetry for electroweak and strong interactions or the approximate global flavor symmetry of quarks. In contrast, the symmetry-unified dynamics in the condensed matter physics is less explored and appreciated. Despite that, there was an exceptional SO(5) model proposed by Zhang [1] as the unified model of d-wave superconductivity (d-SC) and anti-ferromagnetism (AF). However, in order to explain the phase diagram of high temperature (high T_c) superconductivity one needs to add the explicit symmetry breaking terms in this model.

In the context of AdS/CFT correspondence, the global symmetry of the boundary CFT is dual to a gauge symmetry of the bulk gravity. For example, in the study of meson dynamics of the holographic QCD, the flavor symmetry of QCD is dual to the gauge symmetry on the probe mesonic branes [2]. Similarly, in the recent proposal of holographic superconductor [3,4], the global U(1) symmetry for the charge conservation is again dual to a U(1) gauge symmetry in the bulk gravity. These gravity models indeed capture the essential feature of the dual CFTs.

The gauge symmetry usually constrains on the dynamics more than the global one can do. In the context of AdS/CFT, this could imply that the constraint on the dynamics due to a speculated bulk gauge symmetry might uncover some emergent IR phenomenon of the dual CFT. One can then imagine that some originally disjoint flavor symmetries could be unified into a non-Abelian one at low energy due to the direct or indirect couplings among the various flavor currents. A typical example is the aforementioned SO(5) superconductor, in which the symmetry could be thought as an enlarged emerging symmetry at low energy by merging AF's SO(3) and d-SC's U(1). Motivated by this model and the emerging symmetry principle, it is then tempting to formulate a holographic model of high T_c superconductivity based on some underlying non-Abelian gauge symmetry.

Naively, we can consider the gauge fields and the fundamental scalar under SO(5) gauge symmetry in the AdS–Schwarzschild background as the holographic dual to Zhang's unified theory of high temperature superconductors. We may then ask if it is possible for the black hole to grow the non-Abelian hairs by tuning the asymptotic values of the gauge fields, i.e., the corresponding chemical potentials for the dual flavor charge carriers. If so, one may wonder if it is possible to reproduce the peculiar phase diagram of the high T_c superconductors. However, a quick thought will turn down the proposal. This is because the phase diagram of the high Tc superconductor shows the competition between the anti-ferromagnetic order and the d-wave superconducting order, which is in conflict with the picture of coherent orders dictated by the underlying gauge symmetry. Here, by coherent orders we mean that different order parameters will influence each other to condense at the same temperature. This is in clear contrast with

* Corresponding author.
E-mail addresses: 896410093@ntnu.edu.tw (C.-Y. Huang), linfengli@phy.ntnu.edu.tw (F.-L. Lin), debu@phys.ntu.edu.tw (D. Maity).

0370-2693
doi:10.1016/j.physletb.2011.08.053

the competing order phenomena in high T_c superconductivity. Indeed, in [1] one needs to add the explicit SO(5) breaking terms in order to achieve the phase diagram with competing orders. Translated into the gravity dual picture, one needs to break the SO(5) gauge symmetry explicitly, which will usually lead to inconsistence as for massive gauge theories not via Higgs mechanism.

We will not consider the complicated broken SO(5) case. As a first step, we believe that the superconductivity with coherent orders is also an interesting physical phenomena to look into. We can introduce a non-Abelian gauge symmetry in the bulk to describe coherent orders of the boundary field theory. The coherent orders are arising from the condensation of the different kind of charge carriers. In the holographic QCD, these non-Abelian gauge fields are well known to be holographically dual to the quark or meson flavors. Similarly, we will interpret different component of the non-Abelian gauge field to be the holographic dual to some current associated with the different band carriers. From the usual AdS/CFT dictionary, asymptotic boundary values of the gauge fields will be dual to the chemical potentials of the corresponding band carriers. Unified non-Abelian symmetry can be understood as an emergent global symmetry due to the nontrivial interactions among the different band carriers. This is the origin of the coherent orders.

It is interesting to mention that there indeed exist the real multi-band superconductors such as Magnesium diboride (MgB_2) [5,6] and the recently discovered iron pnictides [7]. The MgB_2 does show the coherent orders in its superconducting ground state. More specifically, it has two energy gaps for two different band carriers with the same critical temperature T_c. However, there is no clear physical understanding why the coherent orders occur. Our study provides a clue to explain it by the underlying non-Abelian symmetry.

In this Letter, we will study the most simplest non-Abelian symmetric holographic multi-band superconductor, namely the model based on a bulk SO(3) gauge symmetry. The appearance of the multiple energy gaps with the same T_c is an interesting outcome of this Letter. Our results also show that a sub-sector of this model reproduce the coherent orders of the 2-band superconductor. This may imply that the underlying dynamics of MgB_2 superconductor has a hidden SO(3) symmetry at low energy. Beside these, the phase diagram for the full 3-band case also shows interesting feature. At this point we would like to remind the readers that our model is different from holographic p-wave superconductors considered in [8], where only the non-Abelian gauge fields are introduced, not the fundamental scalars.

We would like to emphasize that the motivation for the holographic study of the condensed matter systems is to uncover the universal behaviors of the systems, especially the ones dictated by the underlying symmetries. For examples, the U(1) symmetry is important for the holographic s-wave superconductor [3] to have the mean-field like behavior, the SU(2) symmetry is crucial for the holographic p-wave superconductor [8], and the near horizon $1+1$ conformal symmetry can explain the peculiar behavior of the holographic non-Fermi metals [9]. Again our holographic SO(3) model can explain the appearance of the coherent orders. This is also beyond the scope of the holographic U(1) model. Therefore, our result implies that the appearance of the coherent orders are universal in the system with non-Abelian symmetry among different band carriers.

The coherent orders in the real multi-band materials such as MgB_2 are believed to be due to the phonon coupling between the different band carriers, and can be obtained from the first principle calculation based on some microscopic models [10]. However, in this kind of approach it usually needs fine-tuning of the model parameters, and lacks the physical understanding of the underlying dynamics. In this regard, our SO(3) holographic model provides the physical insight for the underlying dynamics of the coherent orders, namely, it is dictated by the emergent SO(3) symmetry among the different band carriers. Though our result holds for the strong dynamics based on its gravity dual, it should also hold for the weak coupling regime as long as the same SO(3) symmetry emerges there. The strength of the coupling will only affect the mean-field behavior quantitatively, but not qualitatively. Indeed, we will see this is the case as in the holographic U(1) superconductor. Our finding may trigger in searching for the new strongly correlated materials which are unconventional superconductor with multiple order parameters and have the same critical temperature.

Another interesting challenge for our proposal is how to identify the physical electromagnetic $U(1)_{EM}$ in order to calculate the holographic conductivity. Naively, the $U(1)_{EM}$ could be the Cartan sub-algebra of SO(3). However, there is no unique choice since the arbitrary proper linear combination of the SO(3) generators will play the equivalent role. We need to find some additional criterion for such an identification. In analogy to QCD, the flavored SO(3) current is usually different from the electric current, and the latter should be invariant under the rotation associated with the flavor symmetry. In this way, we will identify the bulk field which is dual to the $U(1)_{EM}$, and then evaluate the corresponding holographic conductivity.

The Letter is organized as follows. In the next section we will pull out the equations of motion for the gauge fields and fundamental scalars, and give proper holographic interpretation. In Section 3 we numerically solve the equations of motion for the background fields in the probe limit, and display the phase diagrams for the holographic multi-band superconductor. In Section 4 we identify a gauge-invariant Cartan sub-algebra as the physical U(1) coupled to photon, and evaluate the corresponding holographic conductivity. Finally we briefly conclude our Letter in Section 5. In Appendix A, we give the numerical results for the SO(3) conductivity matrix.

2. SO(3) in AdS–Schwarzschild background

As we have already mentioned in the Introduction, we will consider SO(3) gauge fields and fundamental scalars in the AdS–Schwarzschild black hole background. The scalars are the holographic duals to the superconducting order parameters of the boundary theory. The dual boundary global symmetry can be thought of as enlarged unified symmetry of multiple U(1) order parameters of some superconductors with multi-band carriers, e.g., the 2- or 3-band superconductors. Microscopically, the unification of the symmetry could arise from the indirect interaction among the different band carriers via the phonon coupling. As we will see, our model reproduces the coherent feature of the order parameters for the 2-band superconductors, and this may justify the hidden SO(3) symmetry of the underlying unified dynamics for the 2-band carriers.

The action for our holographic multi-band superconductor model is

$$S=\int d^4x\sqrt{-g}\left(R+\frac{6}{L^2}-\frac{1}{8}\operatorname{Tr}F_{\mu\nu}^2-|D_\mu\phi|^2-m^2\phi^2\right),\quad(2.1)$$

where the scalar ϕ is in the fundamental representation of SO(3), i.e., $\phi=(n_3,n_2,n_1)^T$, and the covariant derivative $D_\mu\phi:=\partial_\mu\phi-iqA_\mu\phi$. q is the Yang–Mills gauge coupling parameter. The gauge connection A_μ is in the adjoint representation, i.e.,

$$A_\mu=i\begin{pmatrix}0&-A_\mu^1&-A_\mu^2\\A_\mu^1&0&-A_\mu^3\\A_\mu^2&A_\mu^3&0\end{pmatrix}\equiv\sum_{i=1}^{3}A_\mu^i\tau^i,\quad(2.2)$$

where the τ^i's are Hermitian SO(3) generators obeying the SO(3) Lie algebra, i.e.,

$$\left[\tau^i\tau^j\right] = if^{ijk}\tau^k, \qquad \mathrm{tr}\left(\tau^i\tau^j\right) = 2\delta^{ij}. \tag{2.3}$$

Here f^{ijk}'s are the structure constants of the SO(3) Lie algebra, i.e., $f^{123} = f^{231} = f^{312} = 1$, etc. The explicit representations of τ_i's can be read from (2.2). The field strength is then given by

$$F^i_{\mu\nu} \equiv \partial_\mu A^i_\nu - \partial_\nu A^i_\mu + qf^{jki}A^j_\mu A^k_\nu \tag{2.4}$$

or in more compact form $F_{\mu\nu} \equiv F^i_{\mu\nu}\tau^i = \partial_\mu A_\nu - \partial_\nu A_\mu - iq[A_\mu A_\nu]$.

The gauge field A^i_μ is the holographic dual of the current J^i_μ consisting of the carriers in the i-th band, and the scalar field n^i is dual to the mean field order operator $O^{(i)}$ in the i-th band. The SO(3) symmetry is the aforementioned unification of three U(1) bands of the carriers due to some microscopic dynamics such as phonon coupling. From the action (2.1) we can derive the equations of the motion. The equation of motion for ϕ is

$$\frac{1}{\sqrt{-g}}\partial_\mu\left(\sqrt{-g}D^\mu\phi\right) - iqA^\mu D_\mu\phi - m^2\phi = 0. \tag{2.5}$$

The equation for A^i_μ is

$$\begin{aligned}&\frac{1}{\sqrt{-g}}\partial_\mu\left(\sqrt{-g}F^{i\mu\nu}\right) + qf^{ijk}A^j_\mu F^{k\mu\nu}\\ &\quad = iq\left[\phi^T\tau^i D^\nu\phi - \left(D^\nu\phi\right)^T\tau^i\phi\right].\end{aligned} \tag{2.6}$$

To mimic the dual superconductor, we should put the probe gauge fields and scalar on a bulk black hole background with the standard AdS–Schwarzschild metric

$$ds^2 = -f(r)\,dt^2 + \frac{dr^2}{f(r)} + r^2\left(dx^2 + dy^2\right) \tag{2.7}$$

where $f(r) = \frac{r^2}{L^2} - \frac{M}{r}$. As usual, the temperature of the black hole is $T = \frac{3M^{1/3}}{4\pi L^{4/3}}$, which is also the temperature of the dual boundary theory.

We now consider the probe background gauge fields as following

$$A_\mu\,dx^\mu := \left[\Pi_1(r)\tau^1 + \Pi_2(r)\tau^2 + \Pi_3(r)\tau^3\right]dt, \tag{2.8}$$

and the background scalar field configuration

$$\phi := \left(n_3(r), n_2(r), n_1(r)\right)^T. \tag{2.9}$$

Note that the ordering is the reverse of the conventional one to make its compatible with the labeling for the gauge field.

The equations of motion for $n_i(r)$ are

$$n_i'' + \left(\frac{f'}{f} + \frac{2}{r}\right)n_i' + \frac{q^2}{f^2}(\Pi n)_j\frac{\partial(\Pi n)_j}{\partial n_i} - \frac{m^2}{f}n_i = 0, \tag{2.10}$$

for $i, j = 1, 2, 3$. In the above we have defined the bracket vectors as follows,

$$\begin{aligned}&(AB)_1 = -(A_1B_2 + A_2B_1), \qquad (AB)_2 = A_1B_3 - A_3B_1,\\ &(AB)_3 = A_2B_3 + A_3B_2.\end{aligned} \tag{2.11}$$

The equations of motion for $\Pi_i(r)$ are

$$\Pi_i'' + \frac{2}{r}\Pi_i' - \frac{2q^2}{f}(\Pi n)_j\frac{\partial(\Pi n)_j}{\partial\Pi_i} = 0, \tag{2.12}$$

along with the first order gauge constraints due to our ansatz (2.8)

$$\begin{aligned}&\mathcal{R}_1 = \left(\Pi_2\Pi_3' - \Pi_2'\Pi_3\right) - 2f\left(n_3n_2' - n_3'n_2\right) = 0,\\ &\mathcal{R}_2 = \left(\Pi_1\Pi_2' - \Pi_1'\Pi_2\right) - 2f\left(n_2n_1' - n_2'n_1\right) = 0,\\ &\mathcal{R}_2 = \left(\Pi_3\Pi_1' - \Pi_3'\Pi_1\right) - 2f\left(n_3n_1' - n_3'n_1\right) = 0.\end{aligned} \tag{2.13}$$

In order to solve the equations of motion, we require the above gauge constraints to be consistent with the equations of motion. This will yield a consistent set of boundary conditions for the gauge fields and scalar fields at horizon. To see this, we consider the proper combination of the field equations (2.10) and (2.12). One can easily see that out of the combinations of these six equations, there are three independent equations as follows

$$\mathcal{R}_i' + \frac{\mathcal{R}_i}{r} = 0 \quad\Longrightarrow\quad \mathcal{R}_i = \frac{C_i}{r^2} \tag{2.14}$$

where $i = 1, 2, 3$, and C_i's are the integration constants. So, in order to be consistent with the constraint equations (2.13), the above three integration constants should be zero. This will impose the boundary conditions for the gauge and scalar fields at the black hole horizon. One such a consistent set of boundary conditions would be to have vanishing gauge fields and regularity of the scalar fields at the horizon. Interestingly, this is precisely the set of boundary condition which we usually consider in the holographic set up. With these above mentioned choice of conditions, we can solve the equation of motions without worrying about the constraint equations.

At this point, it is important to note that we can reduce this 3-band model to a 2-band one by setting one of the following pairs to zero, (n_1, Π_1), (n_2, Π_2) or (n_3, Π_3). We can further reduce to the familiar U(1) model by setting two of the above pairs to zero. These relations imply that the multi-band models are deeply related to the U(1) case. We will see this is indeed the case by the similarity of the phase diagrams.

On the other hand, we cannot reduce a 3-band configuration to a 2- or 1-band configuration by gauge transformation. The reason is that the vacuum is Higgsed and the gauge symmetry is broken so that the configurations connected by the gauge transformation will have different energies, and cannot be physically equivalent. This can be checked explicitly by showing that one cannot reduce the number of non-zero gauge fields and the scalars for a given configuration at the same time by gauge transformation. This holds even we just perform the global transformation at asymptotic infinity.

3. Phase diagrams

In this section, we will solve the equations of motion (2.10)–(2.12) by the numerical shooting method, and find out the phase diagrams. Note that there are 6 functions to be solved so that we write a Fortran program of shooting method to perform such a task.

As usual, we need to impose the boundary conditions to solve the equations of motion. Moreover, the chosen boundary conditions should be also consistent with the gauge constraints (2.13). After manipulating the combinations of the gauge constraints, we find that the consistent boundary conditions are pretty much the same as the ones for the holographic U(1) superconductor with vanishing gauge fields and regularity of the scalar fields at the black hole horizon, namely, at the horizon $r = r_0$, $\Pi_i = 0$ so that $\Pi_i\,dt$ has finite norm, and the equations of motion for n_i implies $n_i = 3r_0n_i'/m^2L^2$.

Hereafter, we will choose $L = 1$ and $m^2 = -2$ so that n_i is dual to a CFT operator $\mathcal{O}^{(i)}$ with conformal dimension 1 or 2. This yields the following asymptotic behaviors at $r = \infty$,

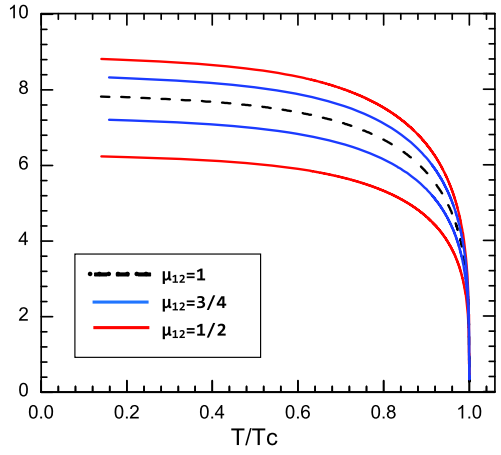

Fig. 1. $\frac{\sqrt{\langle\mathcal{O}_2^{(i)}\rangle}}{T_c}$ vs. $\frac{T}{T_c}$, $i=1,2$ — the phase digram for the holographic 2-band superconductor, which is only a function of $\mu_{12}:=\frac{\mu_1}{\mu_2}$. We show the cases with $\mu_{12}=1,3/4,1/2$.

$$n_i=\frac{n_i^{(1)}}{r}+\frac{n_i^{(2)}}{r^2}+\cdots, \tag{3.1}$$

$$\Pi_i=\mu_i-\frac{\rho_i}{r}+\cdots. \tag{3.2}$$

From the above we can read off the properties of the dual CFT, i.e., the condensate of the operator $\mathcal{O}^{(i)}$ is given by

$$\langle\mathcal{O}_a^{(i)}\rangle=\sqrt{2}n_i^{(a)},\quad a=1,2 \tag{3.3}$$

with $\epsilon_{ab}n_i^{(b)}=0$. For simplicity, we only consider the case of $a=2$ in this Letter. The value of $\langle\mathcal{O}_2^{(i)}\rangle$ at zero temperature is the energy gap for the i-th band carrier to form the BCS-like Cooper pairs, and the values of μ_i and ρ_i are the chemical potential and the carrier density of the i-th band carriers, respectively.

Since the 2-band superconductor is well studied by the experiments, we will first focus on the 2-band case of our model by setting $n_3=\Pi_3=0$, i.e., we will consider only the pairs (n_1,Π_1) and (n_2,Π_2). The phase diagram from our numerical result is shown in Fig. 1. We see that the phase diagram in terms of the dimensionless quantities is universal, and is only function of μ_1/μ_2. More importantly, the phase diagram shows coherent orders, and each order parameter obeys the BCS-like universal scaling behavior, i.e., the carriers of 2 bands condense at the same T_c with the universal critical behavior as the real MgB2 2-band superconductor does [6]. By the numerical fitting, we find

$$\langle\mathcal{O}_2^{(i)}\rangle\simeq 163T_c^2\frac{\mu_i}{\sqrt{\mu_1^2+\mu_2^2}}\left(1-\frac{T}{T_c}\right)^{1/2},$$
$$i=1,2 \text{ for } T\simeq T_c. \tag{3.4}$$

This is in contrast to the case for U(1) holographic superconductor, $\langle\mathcal{O}_2\rangle\simeq 144T_c^2(1-\frac{T}{T_c})^{1/2}$. However, in both cases we all have the mean-field critical exponent $\beta=1/2$.

Moreover, the scaling relation between T_c and the carriers' densities is as follows from the numerical fitting

$$T_c\simeq 0.118\sqrt{\rho_1^2+\rho_2^2}. \tag{3.5}$$

This is in analogy to the one for the U(1) case, i.e., $T_c\simeq 0.118\rho^{1/2}$.

Up to now, our results of the phase diagram agree well with the BCS-like behavior for the 2-band superconductor, it could be the strongly coupled version of the ordinary 2-band superconductor.

Now we turn on all 3 bands at the same time, numerically we find that the results are more sensitive to the intrinsic numerical errors as expected. The phase diagrams show the similar mean-field feature as the 2-band case. Some of the typical phase diagrams are shown in Fig. 2. It is interesting to see that by tuning the chemical potentials μ_i, one can collapse the 3 bands into 2-band or 1-band cases. Moreover, there is a inversion of the vevs or the energy gaps as shown in Fig. 2(a) and (c).

As noted, the temperature dependence of the $\langle\mathcal{O}_2^{(i)}\rangle$'s near the critical point still conforms to the mean-field behavior, however, the chemical potential dependence is far more complicated than (3.4) for the 2-band case. We cannot find the complete dependence on the chemical potentials, but just the proportionality relation as follows:

$$\langle\mathcal{O}_2^{(i)}\rangle=C_iT_c^2\left(1-\frac{T}{T_c}\right)^{1/2},\quad i=1,2 \text{ for } T\simeq T_c, \tag{3.6}$$

with

$$C_1:C_2:C_3=\frac{2\mu_2|\mu_3-\mu_2|}{|\mu_1-\mu_2|+|\mu_3-\mu_2|}:\mu_1+\mu_3$$
$$:\frac{2\mu_2|\mu_1-\mu_2|}{|\mu_1-\mu_2|+|\mu_3-\mu_2|}. \tag{3.7}$$

On the other hand, the scaling relation between the critical temperature and the carriers' densities has the similar form as the 2-band and the U(1) cases, namely,

$$T_c\simeq 0.118\sqrt{\rho_1^2+\rho_2^2+\rho_3^2}. \tag{3.8}$$

So far we have discussed about the superconducting phase diagram of a holographic multi-band superconductor. Behavior of the condensation for each band is universal in terms of temperature. As we decrease the temperature, condensation happens at the same temperature for all the band carries. As we have mentioned in the introduction this phenomena is quite similar to the real two-band superconductor MgB_2. In the subsequent section we will calculate the superconducting transport properties like optical conductivity under small electromagnetic perturbation.

4. Holographic conductivity

In this section, we would like to derive the field equations for the gauge field perturbation on the above background. We then solve these equations to obtain the holographic real time Green functions of boundary currents, from which we can extract the conductivities.

Let us turn on the gauge field perturbation of the x-component as follows,

$$\delta A_\mu\,dx^\mu:=e^{-i(\omega t-k_2y)}\left[a_1(r)\tau^1+a_2(r)\tau^2+a_3(r)\tau^3\right]dx. \tag{4.1}$$

Plugging the perturbed fields into the field equations (2.6), and expand it up to the linear order, from which we can derive the field equations for the perturbed fields. The results are the following,

$$a_i''+\frac{f'}{f}a_i'+\frac{1}{f^2}\big(\omega^2a_i+2iq\omega f^{ijk}\Pi_ja_k$$
$$+q^2(\vec{\Pi}\cdot\vec{\Pi}a_i-\Pi_i\vec{\Pi}\cdot\vec{a})\big)$$
$$-\frac{1}{f}\left(2q^2(an)_j\frac{\partial(an)_j}{\partial a_i}+\frac{k_2^2}{r^2}a_i\right)=0, \tag{4.2}$$

where we define $\vec{\Pi}:=(\Pi_1,\Pi_2,\Pi_3)$, $\vec{a}:=(a_1,a_2,a_3)$, and the inner product such as $\vec{\Pi}\cdot\vec{a}=\Pi_1a_1+\Pi_2a_2+\Pi_3a_3$. In the above expressions, we have again used the bracket notation defined in (2.11).

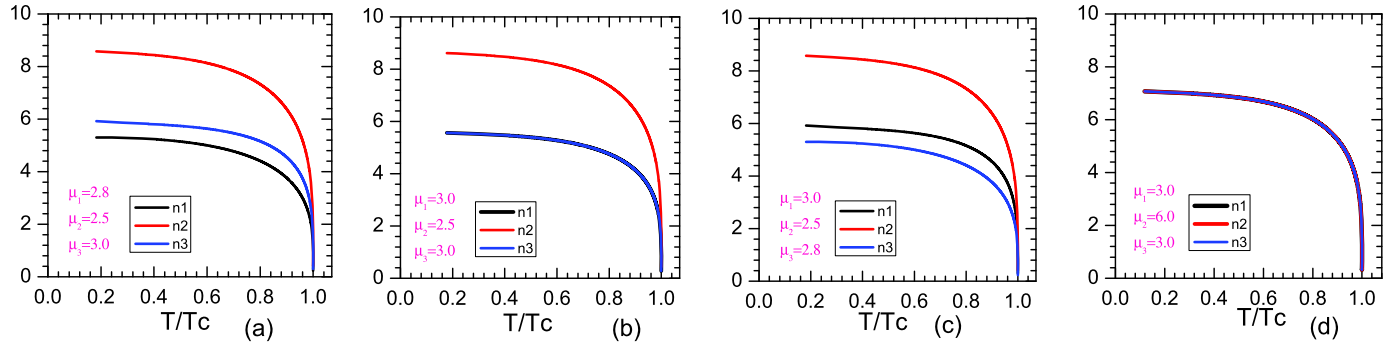

Fig. 2. $\frac{\sqrt{\langle \mathcal{O}_2^{(i)} \rangle}}{T_c}$ vs. $\frac{T}{T_c}$, $i = 1, 2, 3$ — the phase digram for the holographic 3-band superconductor. We show the band-gap competition by tuning the chemical potentials.

We also have noticed that there is no constraint equations among a_i's perturbations as long as we consider a specific form (4.1) of the electromagnetic perturbation. Therefore, from the holographic point of view the external electric field at the boundary does not produce any scalar perturbation in our background.

Similar to the Abelian case, we then solve the above equations by imposing the incoming wave boundary condition in the near horizon region, namely $a_i = f^{-i\omega L^2/3r_0}[1 + a_{i,1}(r - r_0) + \cdots]$. Then from the asymptotic behavior of all the fields at the asymptotic boundary we found

$$a_j(r, \vec{k}, \omega) = a_j^{(0)}(\vec{k}, \omega) + \frac{a_j^{(1)}}{r}(\vec{k}, \omega) + \cdots. \tag{4.3}$$

It then seems that one can evaluate the holographic conductivity by the standard holographic prescription for the Ohmic law [11–14]. However, one should be careful about the fact that all the perturbed fields a_i's are linearly coupled to each other in the bulk. This coupling among the fields implies that source of one particular perturbed field will also source the current corresponding to the other components. If we identify a_i as dual to the U(1) current for the i-th band, this will then yield

$$\langle J_i \rangle = \sigma_{ij} E_j, \tag{4.4}$$

with 3×3 matrix σ_{ij} as a general conductivity matrix in the global SO(3) space. Noe that the i, j are the indices for the SO(3) internal space, not the space–time ones. Since the conductivity matrix cannot be measure directly, we will not discuss it further here but in Appendix A.

In our model we have three different kinds of carriers corresponding to three components of a fundamental scalar field in the bulk. Each carrier has the corresponding boundary current dual to a_i. This dual current transforms like a vector under the global internal symmetry. This is, however, not the current that we are interested in. Now how do we define the conductivity under U(1) electromagnetic field? According to the standard holographic prescription, the above currents are actually some kind of weekly gauged flavor currents similar to the standard s-wave superconductor. As we have argued, the system we are considering is a holographic multi-band superconductor. So, all the band carriers should couple to a single physical photon field through which we will calculate the optical conductivity of the system.

Naively, we can identify one of the three generators of SO(3) as the physical $U(1)_{EM}$, namely the Cartan subalgebra, and the other two as the ladder operators. More specifically,

$$[\tau^3, \tau^\pm] = \pm\tau^\pm, \qquad [\tau^+, \tau^-] = \tau^3. \tag{4.5}$$

However, the above identification is not unique, and any linear combination of the three SO(3) generators with proper normalization will play the same role. Even though there is an arbitrariness in defining the U(1) subgroup, any physical quantity should be independent of that particular choice. But this does not happen in our case. Specifically, considering above particular definition, we can find out the solution for a_3 which coupled to a boundary current with the source of physical electric field, but other two components a_1 and a_2 are sourceless or normalizable. Then one can calculate σ_{33} and identify it as a physical conductivity using the standard holographic prescription. This is how we indeed calculated the conductivity matrix as shown in Fig. 5 of Appendix A. We can apply the same procedure for the other choice of U(1), but those choices lead to different values of the conductivity as one can easily see from the plot for the conductivity matrix. This discrepancy is intuitively obvious because the background chemical potential for each band carrier is different. So, when we consider different choice of U(1) subgroup of the bulk gauge group, we are actually not considering same photon field at the boundary.

Therefore, the Cartan subgroup cannot be the physical $U(1)_{EM}$ for the electromagnetism. Instead, the physical U(1) electric current should be independent of the choice of the Cartan subalgebra, invariant under the global SO(3) rotation and also does not depend on the intrinsic properties of the individual band carrier. We therefore can interpret that particular combination as a dual to the physical $U(1)_{EM}$ current at the boundary. Accordingly, we can evaluate the holographic conductivity which is invariant under the SO(3) transformation and also does not depend on individual chemical potential.

It seems strange that the physical $U(1)_{EM}$ current is defined only for the perturbation but not for the background. However, in the holographic approach this is natural because the background gauge field is dual to the chemical potential and carriers' density, which define the properties of the vacuum not the dynamics. In fact, the different band carriers should have the corresponding chemical potentials and carriers' densities as specified by the background profiles. In contrast, the perturbation of the gauge field is dual to the electric source and the dynamical current in the context of linear response theory. In this case, all the carriers are coupled to the same $U(1)_{EM}$ source, and an unambiguous identification of physical $U(1)_{EM}$ is necessary.

Mapping the above consideration back to the bulk point of view, the SO(3) rotation is translated into the gauge transformation for the total gauge field, namely,

$$\delta A_\mu^i = \partial_\mu \alpha^i + q f^{ijk} A_\mu^j \alpha^k \tag{4.6}$$

where the total gauge field A_μ^i includes both the background ansatz (2.8) and the fluctuation one (4.1), and α^i's are the gauge functions. Since we are only interested in the SO(3) rotation relating different choices of Cartan U(1), this implies that the gauge function functions should be independent of the boundary coordinates. This particular class of gauge transformation retain the

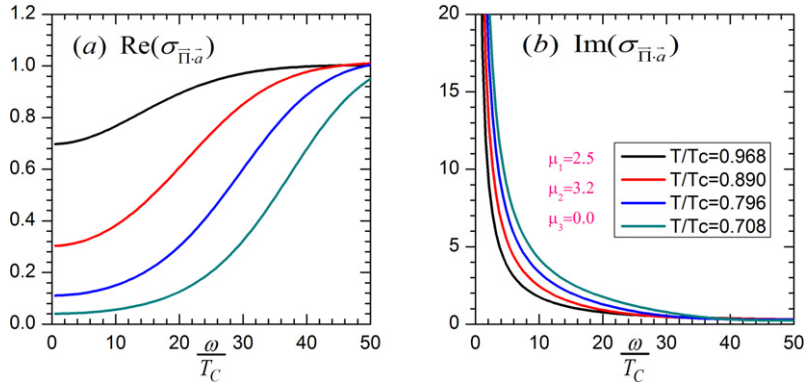

Fig. 3. The AC conductivity $\sigma_{\vec{\Pi}\cdot\vec{a}}$ of 2-band superconductor for $\mu_1 = 2.5$, $\mu_2 = 3.0$, $\mu_3 = 0.0$. (Left): the real part of conductivity, and (Right): the imaginary part.

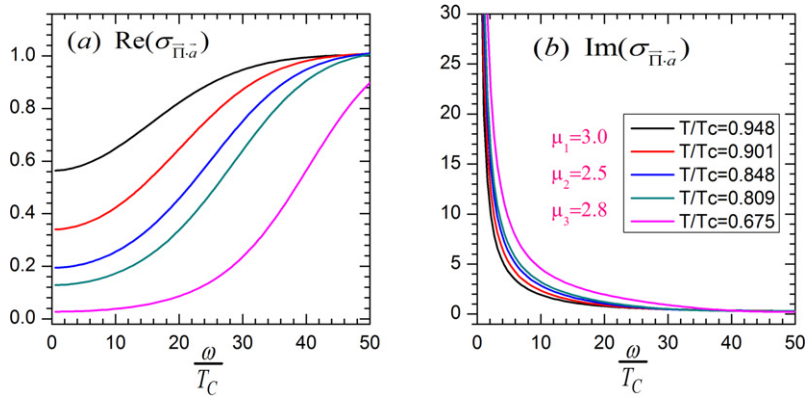

Fig. 4. The AC conductivity $\sigma_{\vec{\Pi}\cdot\vec{a}}$ of 3-band superconductor for $\mu_1 = 3.0$, $\mu_2 = 2.5$, $\mu_3 = 2.8$. (Left): the real part of conductivity, and (Right): the imaginary part.

transformed total gauge field in the same class[1] of the ansatz (2.8) and (4.1) if we also require the gauge functions are also independent of r. Then, the gauge functions become constant gauge parameters and the gauge transformations reduce to the global rotation, and the only nontrivial parts of the transformations are

$$\delta\Pi_i = f^{ijk}\Pi_j\alpha^k, \qquad \delta a_i = f^{ijk}a_j\alpha^k. \tag{4.7}$$

The task to find the dual field of physical U(1)$_{EM}$ is then equivalent to find the appropriate linear combination of the gauge fields a_i's so that it is invariant under the transformation (4.7). it is then straightforward to see the field $\vec{\Pi}\cdot\vec{a}$ satisfies this constraint, and we will identify it as the holographic dual to the physical U(1)$_{EM}$ current. The peculiar dependence of this dual current on the background profile $\vec{\Pi}$ may reflect the physical relevance that the current here is actually the vev of the current operator, which will then depend on the properties of the vacuum encoded in $\vec{\Pi}$.

Accordingly, we can define the holographic conductivity $\sigma_{\vec{\Pi}\cdot\vec{a}}$, and using the asymptotic expansion (4.3) it can be expressed as

$$\sigma_{\vec{\Pi}\cdot\vec{a}} = -\lim_{\vec{k}\to 0}\frac{i\sum_j(\rho_j a_j^{(1)} + \mu_j a_j^{(0)})}{\omega\sum_j \mu_j a_j^{(0)}}. \tag{4.8}$$

Our numerical result for $\sigma_{\vec{\Pi}\cdot\vec{a}}$ for the typical 2- and 3-band cases are shown in Figs. 3 and 4, respectively. We also consider the other cases, including the 2-band one considered in the last section, and the results are similar. We shall also mention that in our numerical calculation we find that $\sigma_{\vec{\Pi}\cdot\vec{a}}$ is independent of the choices of the initial conditions for a_i's at the black hole horizon. This is not so trivial since the perturbed fields a_i's are linearly coupled to each other in the bulk. This property thus supports the identification of $\vec{\Pi}\cdot\vec{a}$ with the dual of U(1)$_{EM}$ current is sensible according to the holographic prescription.

In Figs. 3 and 4, we see that the gap appears clearly in the real part of the total conductivity Re[σ_{tot}] as expected from the Ferrell–Glover sum rule to make up the carriers for the infinite DC conductivity. From the tail near zero frequency, we can extract the density of states for the normal component of the carriers, i.e.,

$$n_n := \lim_{\omega\to 0}\mathrm{Re}\big[\sigma_{tot}(\omega)\big] \simeq C\exp(-\gamma\Delta/T), \tag{4.9}$$

where $\Delta := [\sum_{i=1}^{3}\langle\mathcal{O}_2^{(i)}\rangle^2]^{1/4}/2$.

Moreover, the imaginary part of the total conductivity has a pole at $\omega = 0$. From the Kramers–Kronig relation this implies the infinite DC superconductivity caused by the non-zero superfluidity density, n_s. From our numerics, we can extract the scaling behavior

$$n_s := \lim_{\omega\to 0}\omega\,\mathrm{Im}\big[\sigma_{tot}(\omega)\big] \simeq D(T_c - T) \quad \text{as } T\to T_c. \tag{4.10}$$

The numerical fitting gives $C\sim 14$, $D\simeq 24$ and $\gamma\simeq 0.97$ for the 3-band case, this is the typical mean-field like behavior as for the holographic s-wave superconductor [3]. For the 2-band case, we find the numerical fitting values of C, D and γ are not universal but depend on the chemical potentials. However, we cannot find their dependence on the chemical potentials in the closed form.

5. Conclusion

In this Letter, we study a holographic model which exhibits the low energy behavior of a multi-band superconductor. Specifically, the two-band superconductor like MgB_2 has been studied quite extensively from the theoretical and as well experimental point of

[1] Namely, the background is a time-component of the gauge field as only a function of r, and the perturbation is the x-component of the gauge field.

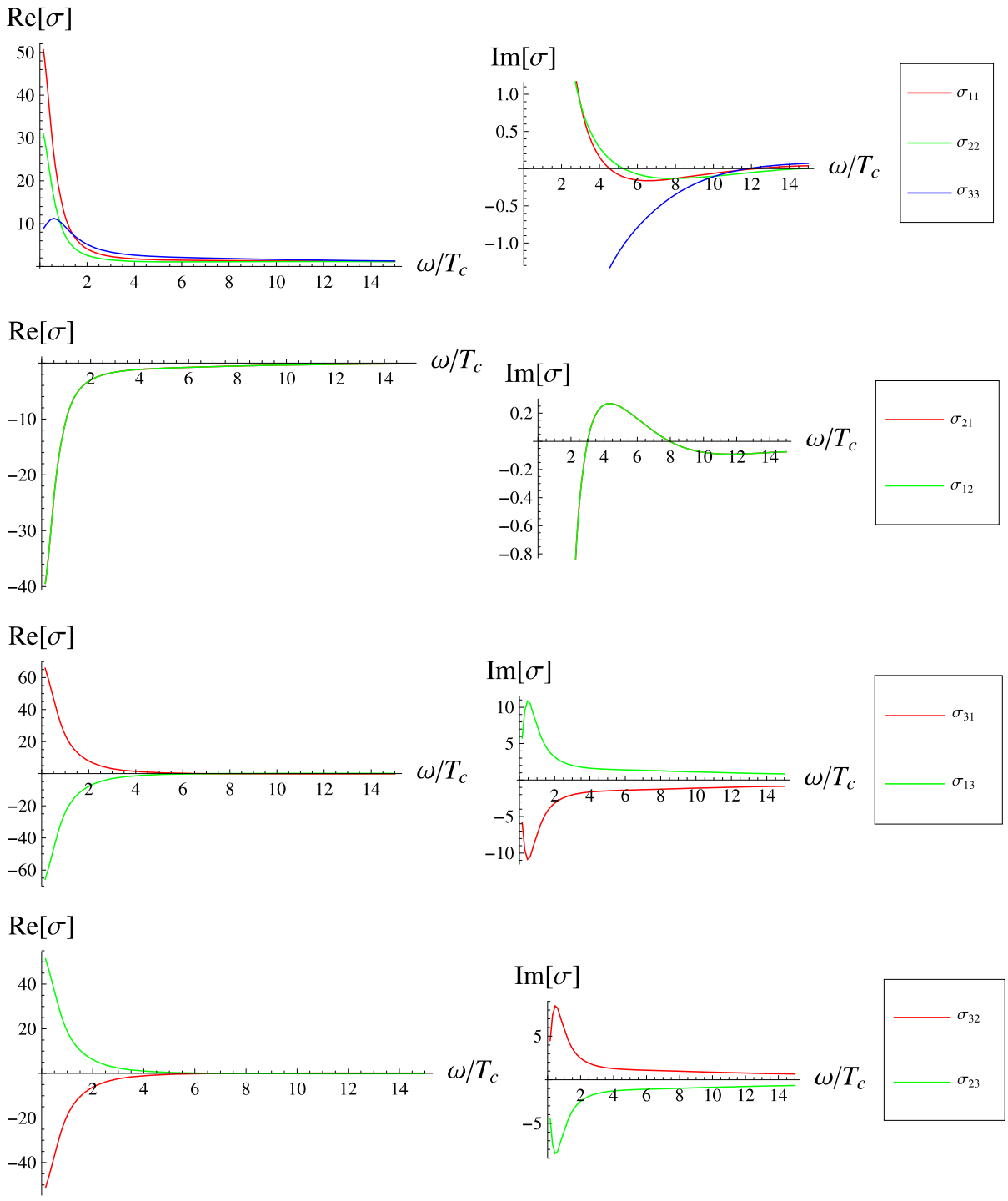

Fig. 5. Conductivity matrix of a 2-band superconductor for $\frac{T}{T_c} = 0.8460$, $\mu_2 = 3.2$, $\mu_3 = 2.5$.

view. Most of the properties of this kind of superconducting material are believed to be explained by the standard BCS theory, however, the insightful understanding for the appearance of the coherent order is obscure in the first principle calculation based on BCS theory. In this report we tried to construct a holographic model of this kind of multi-band superconductor, and attribute the coherent orders to the underlying emergent SO(3) symmetry. We conjectured that the interactions among different band carriers are dictated by an underlying SO(3) global symmetry, which is then dual to the bulk SO(3) gauge dynamics. Surprisingly, our model reproduces the phase diagram with the desirable feature for multi-band superconductor, namely, the feature of the coherent orders. Moreover, we identify a gauge invariant linear combination of the perturbed gauge fields as the dual current coupled to the physical $U(1)_{EM}$ photon, and it shows the mean field BCS-like behavior for the holographic conductivity. However, it deserves further study to clarify the physical subtlety of such an identification, especially its dependence on the background profile. Finally, it is a natural next step to see if these features remain intact after taking into account the back reaction of the bulk fields to the background geometry.

Acknowledgements

We thank Chen-Pin Yeh for taking part in this project at its early stage. We also thank Juinn-Wei Chen, Christopher Herzog and Logan Wu for helpful discussions. This work is supported by Taiwan's NSC grant NSC-099-2811-M-003-007-, and partly by NCTS.

Appendix A

The general definition of conductivity matrix is

$$\sigma_{ij}(\omega) = \frac{1}{\omega} \lim_{\vec{k}\to 0} \int d^4x\, e^{i\omega t - ikx} \theta(t) \big\langle \big[J_i(t,x), J_j(0,0) \big] \big\rangle. \tag{A.1}$$

This quantity may not be measured directly in the real experiments since it should be highly nontrivial to tune the electric field among different band carriers. Despite that, the conductivity matrix provide some "microscopic" picture for the holographic multi-band superconductors, and it is interesting to find out its behavior.

By fixing the background (2.8), it is easy to see that gauge field perturbation a_i's are invariant under the infinitesimal gauge transformation, i.e., $\delta a_i = \bar{D}_x \alpha_i$ where $\bar{D}_\mu = \partial_\mu + g\bar{A}_\mu$ is the covariant derivative with respect to the background gauge field $\bar{A}_\mu$, and α_i's are the gauge parameters. Therefore, by using AdS/CFT correspondence, one can define the SO(3)-invariant general conductivity matrix as follows[2]

$$\sigma_{ij}(\omega) = -\lim_{\vec{k}\to 0} \frac{i a_i^{(1)}(\vec{k},\omega)}{\omega a_j^{(0)}(\vec{k},\omega)} \bigg|_{a^{(0)}_{k\neq j}=0}. \tag{A.2}$$

A typical plot for conductivity matrix is shown in Fig. 5 for 2-band holographic superconductor. Note that it does not have the mean-field like behavior.

References

[1] Shou-Cheng Zhang, Science 275 (1997) 1089.
[2] T. Sakai, S. Sugimoto, Prog. Theor. Phys. 113 (2005) 843, arXiv:hep-th/0412141.
[3] S.A. Hartnoll, C.P. Herzog, G.T. Horowitz, Phys. Rev. Lett. 101 (2008) 031601, arXiv:0803.3295 [hep-th].
[4] S.A. Hartnoll, C.P. Herzog, G.T. Horowitz, JHEP 0812 (2008) 015, arXiv:0810.1563 [hep-th].
[5] J. Nagamatsu, N. Nakagawa, T. Muranaka, Y. Zenitani, J. Akimitsu, Nature 410 (6824) (2001) 63.
[6] X.-X. Xi, Rep. Prog. Phys. 71 (2008) 116501.
[7] Y. Kamihara, et al., J. Am. Chem. Soc. 130 (2008) 3296;
Y. Kamihara, et al., J. Am. Chem. Soc. 128 (2006) 10012.
[8] S.S. Gubser, S.S. Pufu, JHEP 0811 (2008) 033, arXiv:0805.2960 [hep-th].
[9] T. Faulkner, N. Iqbal, H. Liu, J. McGreevy, D. Vegh, Holographic non-Fermi liquid fixed points, arXiv:1101.0597 [hep-th].
[10] A.A. Golubov, J. Kortus, O.V. Dolgov, O. Jepsen, Y. Kong, O.K. Andersen, B.J. Gibson, K. Ahn, R.K. Kremer, J. Phys.: Condens. Matter 14 (2002) 1353.
[11] D.T. Son, A.O. Starinets, JHEP 0209 (2002) 042, hep-th/0205051.
[12] N. Iqbal, H. Liu, Fortsch. Phys. 57 (2009) 367, arXiv:0903.2596 [hep-th].
[13] N. Iqbal, H. Liu, Phys. Rev. D 79 (2009) 025023, arXiv:0809.3808 [hep-th].
[14] S.A. Hartnoll, C.P. Herzog, Phys. Rev. D 76 (2007) 106012, arXiv:0706.3228 [hep-th].

[2] This is similar to the treatment for the holographic p-wave superconductor [8].